Vagus nerve stimulation increases stomach-brain coupling via a vagal afferent pathway

Supplementary Information (SI)

Sophie J. Müller[1], Vanessa Teckentrup[1,6], Ignacio Rebollo[2],

Manfred Hallschmid[3,4,5], Nils B. Kroemer*[1,7]

[1] University of Tübingen, Tübingen Center for Mental Health, Department of Psychiatry and Psychotherapy, 72076 Tübingen, Germany

[2] German Institute of Human Nutrition (DIfE), Department of Decision Neuroscience and Nutrition (DNN), Potsdam-Rehbruecke, 14558 Nuthetal, Germany

[3] University of Tübingen, Department of Medical Psychology and Behavioral Neurobiology, 72076 Tübingen, Germany

[4] German Center for Diabetes Research (DZD), 85764 München-Neuherberg, Germany

[5] Institute for Diabetes Research and Metabolic Diseases of the Helmholtz Center Munich at the Eberhard Karls University Tübingen, 72076 Tübingen, Germany

[6] Trinity College Institute of Neuroscience, Trinity College Dublin, Dublin 2, Ireland

[7] University of Bonn, Department of Psychiatry and Psychotherapy, Bonn, Germany

Corresponding author*

Dr. Nils B. Kroemer, nkroemer@uni-bonn.de

Venusberg Campus 1, 53127 Bonn

Twitter: @cornu_copiae

Software for data analysis

For preprocessing of the EGG data, we used the Fieldtrip toolbox for Matlab (Oostenveld et al., 2011). The fMRI data were preprocessed using the standardized FMRIPREP pipeline (https://github.com/poldracklab/fmriprep) v20.1.1 (Esteban et al., 2019) based on Nipype (Gorgolewski et al., 2011) [RRID:SCR_002502] and Nilearn (Abraham et al., 2014) [RRID:SCR_001362]. For parcellation of brain maps, we used an extended version of the Harvard-Oxford atlas (Desikan et al., 2006), which includes the Reinforcement Learning Atlas (https://osf.io/jkzwp/) for extended coverage of subcortical nuclei and the AAL cerebellum ROIs (Tzourio-Mazoyer et al., 2002). We used RStudio v1.2.5 with the ggplot2 package v3.3.2 (Wickham, 2016), including the tidyverse package v1.3, the viridis color package v0.5.1 (Garnier, 2021), the gghighlight package v0.3.2 (https://github.com/yutannihilation/gghighlight/), and the cowplot package v1.1.0 (https://wilkelab.org/cowplot/) for plotting.

Inclusion criteria for participants

Three participants left the study by request before both sessions had been completed. One participant was omitted from this analysis because the stimulation failed to start precisely at the beginning of the stimulation phase of the resting-state fMRI (rs-fMRI) measurement. One participant was excluded due to excessive motion (>50% of the total number of volumes exceeding a framewise displacement of 0.5 mm) in the resting-state fMRI measurement. Nine participants were excluded from analyses as they did not pass rigorous quality control of EGG and fMRI measurements, as described by Rebollo et al. (2018) and Wolpert et al. (2020).

The following criteria had to be fulfilled: 1) 18-50 years of age; 2) BMI range of 18.5-30 kg/m²; 3) no lifetime history of brain injury, cardiovascular diseases, schizophrenia, bipolar disorder, epilepsy, diabetes, or asthma; 4) no implants (e.g. pacemaker, cochlear implant, cerebral shunt; except dental prostheses); 5) within the last 12 months: no severe substance abuse disorder, anxiety disorder (except specific phobia), obsessive-compulsive disorder, trauma- and stressor-related disorder, somatic symptom disorder or eating disorder; 6) no open wounds or impaired skin at electrode site; 7) not pregnant or nursing; 8) eligibility for MR research (i.e., no non-removable metal parts, such as piercings, no tattoos above the neck or larger than 14 cm, no claustrophobia, noise tolerability) (Teckentrup et al., 2021).

fMRI acquisition and preprocessing

Structural T1-weighted images were measured using an MP-RAGE sequence with 176 sagittal slices covering the whole brain, flip angle = 9°, matrix size = 256 × 256 and voxel size = 1 × 1 × 1 mm^3. Field maps were acquired using a Siemens gradient echo field map sequence with short echo time (TE) = 5.19 ms and long TE = 7.65 ms (TE difference = 2.46 ms). rs-fMRI data (10 min. pre-stimulation baseline and 10 min. with concurrent stimulation) were acquired using a T2*-weighted echo-planar imaging (EPI) sequence with a multiband factor of 4, 68 axial slices with an interleaved slice order covering the whole brain (including brain stem), repetition time (TR) = 1.4 s, TE = 30 ms, flip angle = 65°, matrix size = 110 × 110, field of view = 220 × 220 mm^2 and voxel size = 2 × 2 × 2 mm^3. We further obtained data on the respiratory cycle based on the EGG recordings.

For preprocessing, each T1-weighted (T1w) volume was corrected for intensity non-uniformity using N4BiasFieldCorrection v2.1.0 (Tustison et al., 2010) and skull-stripped using antsBrainExtraction.sh v2.1.0 (using the OASIS template). Brain surfaces were reconstructed using recon-all from FreeSurfer v6.0.1 (Dale et al., 1999) [RRID:SCR_001847], and the brain mask estimated before was refined with a custom variation of the method to reconcile ANTs-derived and FreeSurfer-derived segmentations of the cortical gray-matter of Mindboggle (Klein et al., 2017) [RRID:SCR_002438]. Spatial normalization to the ICBM 152 Nonlinear Asymmetrical template version 2009c (Fonov et al., 2009) [RRID:SCR_008796] was performed through nonlinear registration with the antsRegistration tool of ANTs v2.1.0 (Avants et al., 2008) [RRID:SCR_004757], using brain-extracted versions of both T1w volume and template. Brain tissue segmentation of cerebrospinal fluid (CSF), white-matter (WM) and gray-matter (GM) was performed on the brain-extracted T1w using FAST (Zhang et al., 2001) [FSL v5.0.9, RRID:SCR_002823].

Functional data were slice-time corrected using 3dTshift from AFNI v16.2.07 (Cox, 1996) [RRID:SCR_005927] and motion corrected using MCFLIRT (Jenkinson et al., 2002) [FSL v5.0.9]. Distortion correction was performed using fieldmaps processed with FUGUE (Jenkinson, 2003) [FSL v5.0.9]. This was followed by co-registration to the corresponding T1w using boundary-based registration (Greve & Fischl, 2009) with 9 degrees of freedom, using bbregister [FreeSurfer v6.0.1]. Motion correcting transformations, field distortion correcting warp, BOLD-to-T1w transformation and

T1w-to-template (MNI) warp were concatenated and applied in a single step using antsApplyTransforms [ANTs v2.1.0] based on Lanczos interpolation.

Physiological noise regressors were extracted by calculating the average signal inside the anatomically-derived CSF and WM masks across time using Nilearn. Framewise displacement (Power et al., 2014) was calculated for each functional run using the implementation of Nipype. Following the recommendation of Power et al. (2014), we calculated the number of volumes per run which exceed a framewise displacement threshold of 0.5 mm. If more than 50% of the total number of volumes exceed this threshold or less than 5 minutes of data below this threshold remain, the respective subject was excluded from further analyses.

Respiratory cycle data from the EGG electrodes was preprocessed using BrainVision Analyzer (Brain Products, Germany), FieldTrip (Oostenveld et al., 2011) and the PhysIO toolbox (Kasper et al., 2017). In brief, the EGG recordings were read into BrainVision Analyzer and the Scanner Artifact Correction was applied to remove gradient artifacts from the data before submitting exported time series to FieldTrip. As the typical respiratory rate in humans is around 0.3 Hz, the data were downsampled to 50 Hz and bandpass-filtered between 0.1 and 0.6 Hz. The respiratory time series were then read into the PhysIO toolbox and respiratory phase and respiratory volume per time were calculated. By convolution of the respiratory volume per time with the respiration response function (Birn et al., 2008), the toolbox then generated a nuisance regressor for noise correction.

EGG analysis

First, the data was read out and downsampled to 10 Hz using the Fieldtrip toolbox for MATLAB (Oostenveld et al., 2011). Next, we detrended and demeaned the signal before correcting spike and drift artifacts. Then, we separated our recordings corresponding to the performed tasks. For our analyses presented here, we only used the resting-state data, divided into baseline and stimulation phases. We obtained the frequency spectrum of the stomach corresponding to the range between 0.03-0.07 Hz by performing a fast Fourier transform. Previous studies suggest that the gastric frequency is reliably centered around 0.05 Hz in healthy humans (Wolpert et al., 2020), so we used a Cauchy distribution centered around 0.05 Hz to assign peaks close to the expected frequency a weigher weight a priori to improve robustness of peak detection. Then, we conducted a visual quality control to determine the usability of the

data. Our criteria for this were a clearly visible peak in the expected frequency spectrum (0.03-0.07 Hz) with a power ≥15 μV which was congruent across channels and identifiable for both phases (baseline and stimulation). Next, we defined the gastric frequency of each participant based on the strongest usable EGG channel. We prioritized the highest power during the stimulation phase, as long as the same channel was usable in both phases.

Afterward, we bandpass filtered the EGG time series for both phases (baseline and stimulation) around the respective center frequency. We then downsampled the EGG time series according to the fMRI sampling rate (0.714 Hz). Thereafter, we performed a Hilbert transformation to obtain the phase information of the signal.

To calculate *p*-values for the phase-locking values (PLV), we disassociated the temporal structure between the EGG and the BOLD time series, effectively removing meaningful synchrony between the two signals. The EGG signal was shifted by at least one minute to ensure sufficient discrepancy to the empirical PLV. Consequently, time series were shifted 343 times, resulting in 343 shifted PLV per voxel. Each voxel's CPLV was then defined as the mean of all shifted PLV of this specific voxel.

Analysis of gradients

To analyze how taVNS affects the coupling of functional networks, we assigned each brain region within the extended Harvard-Oxford atlas to one of the 7 cortical resting-state networks as published by Yeo et al. (2011) (DMN, ventral and dorsal attention, visual, somatomotor, frontoparietal, limbic) or a subcortical anatomical network (brainstem, midbrain, diencephalon). The assignment was based on the largest overlap between each region defined within the extended Harvard-Oxford atlas and the network maps provided by Yeo et al. (2011). To evaluate which functional networks show the most substantial change after taVNS, we used the *t*-maps resulting from the full factorial models described above and calculated voxel-wise Cohen's d_z as a measure of effect size by dividing the *t*-values by the square-root of the sample size (n=31). Then, we averaged d_z across all voxels assigned to the same network. To assess how the voxels affected by taVNS are positioned in the cortical hierarchy, we assigned each voxel within the *t*-maps of the SPM-models for Stimulation × Time and the correlation with the metabolic state (details described above, maps available on NeuroVault) to one of the first two cortical resting-state gradients (gradient 1: unimodal to transmodal, gradient 2: somatosensory/somatomotor to visual) as published by

Margulies et al. (2016). We then performed two-sample Kolmogorov-Smirnov tests (MATLAB function kstest2) between the standard cortical gradients and the respective distributions during baseline and stimulation to evaluate how taVNS changes large-scale connectivity patterns.

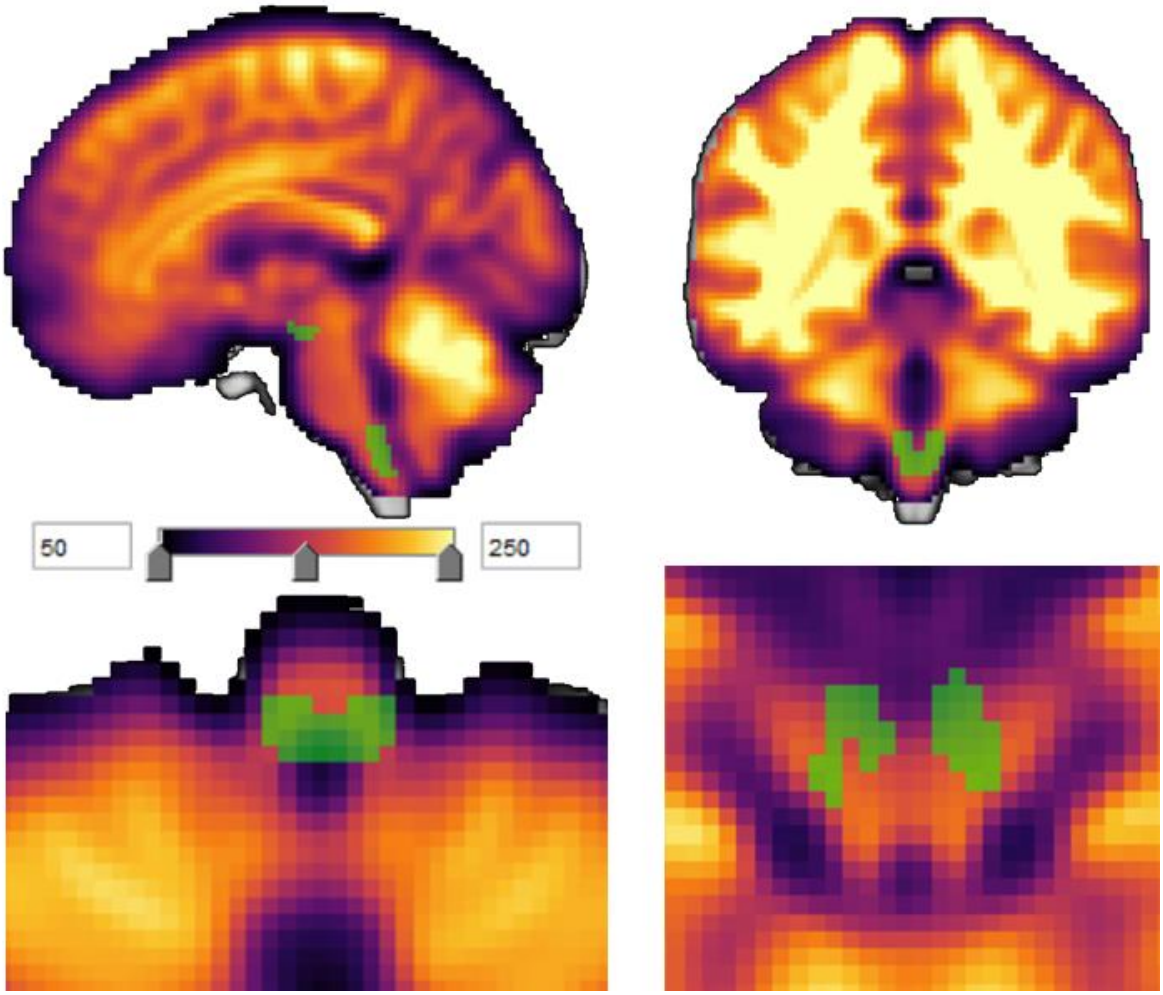

Figure S.1. Temporal signal-to-noise (tSNR) map of the high-resolution sequence (Teckentrup et al., 2021). The selected sections show the primary regions of interest in green: the nucleus of the solitary tract (NTS) and the ventral tegmental area/subtantia nigra. As can be seen in the selected sections, more voxels within the green masks exceed a recommended minimum level of tSNR > 50 with the median voxel close to a tSNR ~150 (Teckentrup et al., 2021). The unthresholded map can be inspected on neurovault: https://neurovault.org/collections/CHANQVEU/

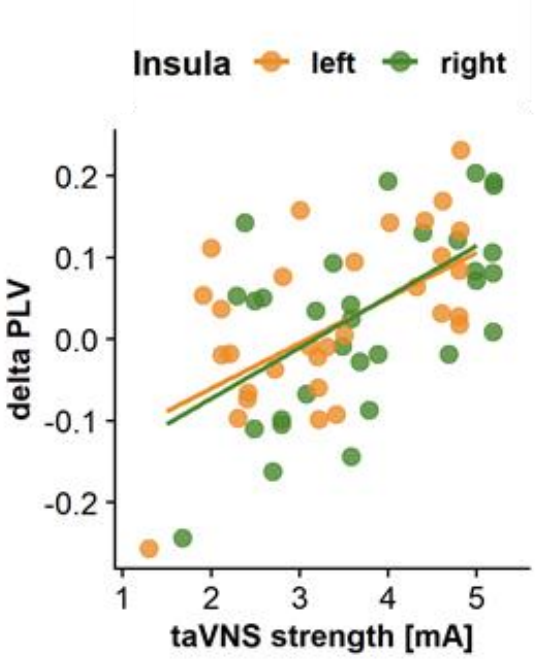

Figure S.2. We found strong positive correlations (r = .58, p < .001) between changes in PLV and taVNS strength in both insular cortices (clusters: right: t_{max} = 4.52, k = 102; left: t_{max} = 4.10, k = 190). This plot shows the extracted PLV changes in relation to the taVNS strength. Each point depicts one participant.

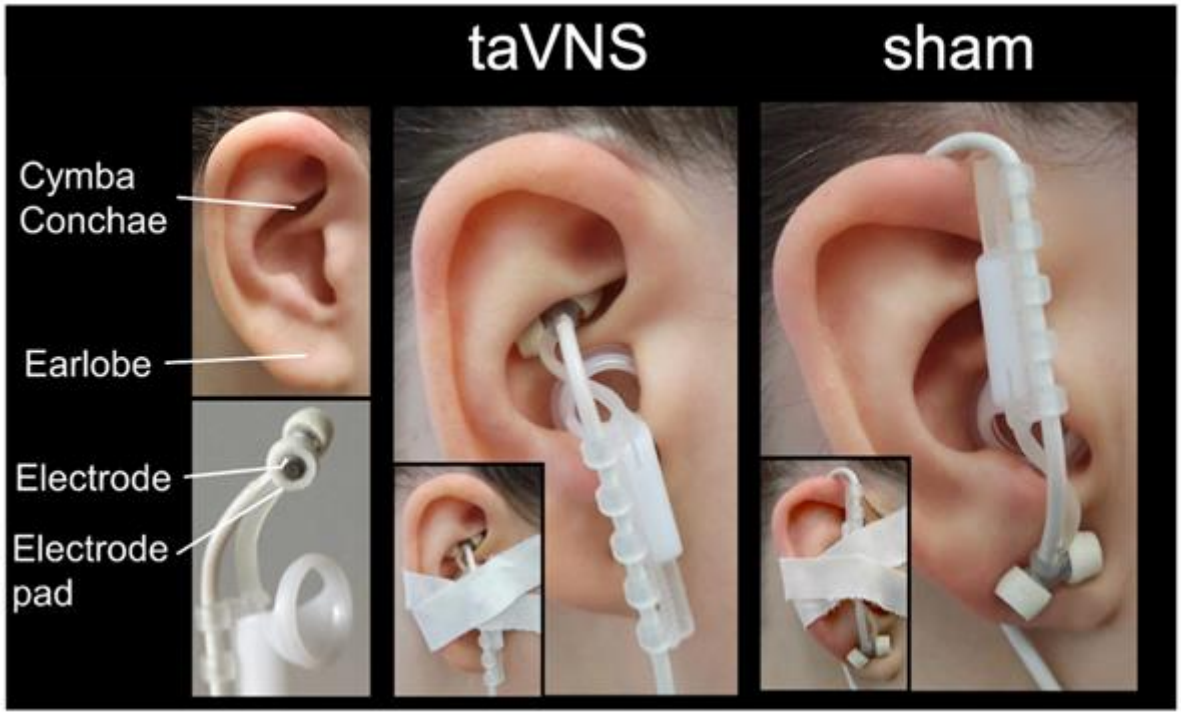

Figure S.3. Placement of the electrode for transcutaneous auricular vagus nerve stimulation (taVNS) and the sham condition.

Table S1. Summary of *t*-values during baseline.

	This study		Rebollo (2018)	
Region (Harvard Oxford Atlas, extended)	**Mean *t***	**Max *t***	**Mean *t***	**Max *t***
FP r (Frontal Pole Right)	0.918	5.104	1.125	5.074
FP l (Frontal Pole Left)	1.312	4.098	1.149	4.633
IC r (Insular Cortex Right)	1.705	4.809	1.421	4.473
IC l (Insular Cortex Left)	1.958	5.38	1.489	4.026
SFG r (Superior Frontal Gyrus Right)	1.133	6.487	1.204	4.895
SFG l (Superior Frontal Gyrus Left)	1.523	5.447	1.3	5.468
MidFG r (Middle Frontal Gyrus Right)	1.49	6.031	1.309	4.298
MidFG l (Middle Frontal Gyrus Left)	1.406	3.677	1.045	3.762
IFG tri r (Inferior Frontal Gyrus, pars triangularis Right)	1.895	4.458	1.306	3.864
IFG tri l (Inferior Frontal Gyrus, pars triangularis Left)	2.001	5.199	1.166	3.686
IFG oper r (Inferior Frontal Gyrus, pars opercularis Right)	2.209	5.933	1.411	3.946
IFG oper l (Inferior Frontal Gyrus, pars opercularis Left)	2.047	4.154	1.025	4.059
PreCG r (Precentral Gyrus Right)	2.362	5.819	1.677	4.525
PreCG l (Precentral Gyrus Left)	2.22	5.931	1.696	4.638
TP r (Temporal Pole Right)	1.14	5.176	1.045	4.669
TP l (Temporal Pole Left)	1.16	4.536	0.874	4.163
aSTG r (Superior Temporal Gyrus, anterior division Right)	1.743	3.746	1.636	4.014
aSTG l (Superior Temporal Gyrus, anterior division Left)	1.19	4.451	1.943	6.074
pSTG r (Superior Temporal Gyrus, posterior division Right)	1.316	2.998	1.77	3.933
pSTG l (Superior Temporal Gyrus, posterior division Left)	0.686	3.151	1.61	3.966
aMTG r (Middle Temporal Gyrus, anterior division Right)	1.14	2.554	1.284	4.153
aMTG l (Middle Temporal Gyrus, anterior division Left)	0.609	3.572	0.979	3.17
pMTG r (Middle Temporal Gyrus, posterior division Right)	0.807	3.3	1.305	4.153
pMTG l (Middle Temporal Gyrus, posterior division Left)	0.708	3.127	0.879	3.703
toMTG r (Middle Temporal Gyrus, temporooccipital part Right)	1.635	4.629	1.114	4.068
toMTG l (Middle Temporal Gyrus, temporooccipital part Left)	1.381	4.663	1.406	3.804
aITG r (Inferior Temporal Gyrus, anterior division Right)	2.094	4.42	1.436	3.631
aITG l (Inferior Temporal Gyrus, anterior division Left)	1.631	4.402	0.703	2.966
pITG r (Inferior Temporal Gyrus, posterior division Right)	1.223	3.902	0.925	3.648

	This study		Rebollo (2018)	
Region (Harvard Oxford Atlas, extended)	**Mean *t***	**Max *t***	**Mean *t***	**Max *t***
pITG l (Inferior Temporal Gyrus, posterior division Left)	1.399	4.398	0.746	4.493
toITG r (Inferior Temporal Gyrus, temporooccipital part Right)	2.04	4.971	1.451	4.259
toITG l (Inferior Temporal Gyrus, temporooccipital part Left)	2.014	5.313	1.544	4.794
PostCG r (Postcentral Gyrus Right)	2.316	5.693	1.893	4.764
PostCG l (Postcentral Gyrus Left)	2.095	5.06	1.824	4.921
SPL r (Superior Parietal Lobule Right)	2.258	4.401	1.736	4.914
SPL l (Superior Parietal Lobule Left)	2.369	5.944	1.554	3.882
aSMG r (Supramarginal Gyrus, anterior division Right)	2.18	4.763	1.587	4.227
aSMG l (Supramarginal Gyrus, anterior division Left)	1.921	4.628	1.63	4.025
pSMG r (Supramarginal Gyrus, posterior division Right)	2.181	4.235	1.166	4.914
pSMG l (Supramarginal Gyrus, posterior division Left)	1.702	4.641	1.225	3.664
AG r (Angular Gyrus Right)	1.454	3.822	1.316	3.824
AG l (Angular Gyrus Left)	1.862	5.06	1.18	3.405
sLOC r (Lateral Occipital Cortex, superior division Right)	1.704	5.205	1.578	5.08
sLOC l (Lateral Occipital Cortex, superior division Left)	1.573	4.719	1.489	4.592
iLOC r (Lateral Occipital Cortex, inferior division Right)	2.204	4.664	1.713	4.479
iLOC l (Lateral Occipital Cortex, inferior division Left)	1.761	3.973	1.545	4.152
ICC r (Intracalcarine Cortex Right)	2.17	4.101	2.204	4.243
ICC l (Intracalcarine Cortex Left)	2.281	4.256	2.107	3.904
MedFC (Frontal Medial Cortex)	0.919	4.159	1.165	3.799
SMA r (Juxtapositional Lobule Cortex- Ri	2.154	5.043	2.132	4.753
SMA L(Juxtapositional Lobule Cortex- Lef	2.341	5.475	1.907	4.274
SubCalC (Subcallosal Cortex)	1.15	3.956	0.871	3.429
PaCiG r (Paracingulate Gyrus Right)	1.453	5.468	1.099	3.374
PaCiG l (Paracingulate Gyrus Left)	1.563	4.429	1.21	3.879
AC (Cingulate Gyrus, anterior division)	2.297	5.892	1.406	6.551
PC (Cingulate Gyrus, posterior division)	1.981	5.765	1.68	4.94
Precuneous (Precuneous Cortex)	2.153	5.792	1.801	4.859
Cuneal r (Cuneal Cortex Right)	1.605	3.916	2.407	4.863
Cuneal l (Cuneal Cortex Left)	1.815	3.422	2.34	4.464
FOrb r (Frontal Orbital Cortex Right)	1.032	4.099	1.328	4.195
FOrb l (Frontal Orbital Cortex Left)	1.28	5.074	1.392	4.543
aPaHC r (Parahippocampal Gyrus, anterior division Right)	1.649	6.599	1.331	3.826
aPaHC l (Parahippocampal Gyrus, anterior division Left)	1.56	5.067	1.067	3.625

	This study		Rebollo (2018)	
Region (Harvard Oxford Atlas, extended)	**Mean *t***	**Max *t***	**Mean *t***	**Max *t***
pPaHC r (Parahippocampal Gyrus, posterior division Right)	1.912	3.826	1.104	3.76
pPaHC l (Parahippocampal Gyrus, posterior division Left)	1.465	3.966	0.936	3.632
LG r (Lingual Gyrus Right)	2.17	5.703	2.17	4.432
LG l (Lingual Gyrus Left)	1.802	4.555	2.131	4.948
aTFusC r (Temporal Fusiform Cortex, anterior division Right)	1.011	4.202	1.594	3.758
aTFusC l (Temporal Fusiform Cortex, anterior division Left)	1.236	3.343	0.957	3.988
pTFusC r (Temporal Fusiform Cortex, posterior division Right)	1.818	4.691	1.218	4.037
pTFusC l (Temporal Fusiform Cortex, posterior division Left)	1.561	3.929	1.063	3.673
TOFusC r (Temporal Occipital Fusiform Cortex Right)	2.555	6.842	1.748	4.243
TOFusC l (Temporal Occipital Fusiform Cortex Left)	2.16	4.111	1.827	4.617
OFusG r (Occipital Fusiform Gyrus Right)	2.563	5.394	1.965	5.206
OFusG l (Occipital Fusiform Gyrus Left)	2.571	5.185	2.026	4.136
FO r (Frontal Operculum Cortex Right)	1.951	4.22	1.417	3.763
FO l (Frontal Operculum Cortex Left)	1.969	4.209	1.145	3.67
CO r (Central Opercular Cortex Right)	2.628	5.149	1.988	4.763
CO l (Central Opercular Cortex Left)	2.181	5.215	1.731	4.112
PO r (Parietal Operculum Cortex Right)	2.193	4.32	1.938	4.209
PO l (Parietal Operculum Cortex Left)	2.544	5.018	2.095	4.084
PP r (Planum Polare Right)	1.992	4.328	1.59	4.006
PP l (Planum Polare Left)	1.97	5.203	1.067	3.08
HG r (Heschl's Gyrus Right)	2.412	4.686	2.111	5.174
HG l (Heschl's Gyrus Left)	2.165	5.051	2.131	5.169
PT r (Planum Temporale Right)	1.789	4.384	2.353	5.285
PT l (Planum Temporale Left)	1.653	4.264	1.998	4.481
SCC r (Supracalcarine Cortex Right)	2.093	3.735	2.246	3.966
SCC l (Supracalcarine Cortex Left)	2.299	4.107	2.208	3.839
OP r (Occipital Pole Right)	1.628	4.62	1.422	4.224
OP l (Occipital Pole Left)	1.638	4.018	1.221	4.074
Thalamus r	2.591	5.601	1.382	3.842
Thalamus l	2.199	5.274	1.461	4.673
Caudate r	0.887	3.136	1.838	4.9
Caudate l	1.365	4.386	1.511	4.326
Putamen r	1.413	3.802	1.21	4.184
Putamen l	1.453	4.286	1.401	4.825
Pallidum r	1.49	4.15	0.88	2.773
Pallidum l	1.842	5.182	0.918	4.057
Hippocampus r	1.586	4.293	1.191	3.727
Hippocampus l	1.649	4.618	0.838	3.465
Amygdala r	1.663	4.042	1.106	3.695

	This study		Rebollo (2018)	
Region (Harvard Oxford Atlas, extended)	**Mean *t***	**Max *t***	**Mean *t***	**Max *t***
Amygdala l	1.618	3.405	0.969	3.625
Accumbens r	1.27	2.827	0.906	2.789
Accumbens l	0.741	2.172	1.556	2.936
Brain-Stem	1.578	6.262	1.039	4.514
Cereb1 l (Cerebelum Crus1 Left)	1.298	4.917	1.675	4.866
Cereb1 r (Cerebelum Crus1 Right)	1.53	4.959	1.417	4.82
Cereb2 l (Cerebelum Crus2 Left)	1.303	5.572	1.513	4.243
Cereb2 r (Cerebelum Crus2 Right)	1.778	4.808	1.13	4.82
Cereb3 l (Cerebelum 3 Left)	1.503	3.538	1.265	3.04
Cereb3 r (Cerebelum 3 Right)	1.658	4.011	1.338	3.592
Cereb45 l (Cerebelum 4 5 Left)	1.626	4.355	1.437	4.72
Cereb45 r (Cerebelum 4 5 Right)	1.683	3.88	1.485	4.003
Cereb6 l (Cerebelum 6 Left)	1.802	4.683	1.669	4.59
Cereb6 r (Cerebelum 6 Right)	2.004	6.336	1.831	4.483
Cereb7 l (Cerebelum 7b Left)	1.881	4.871	0.869	4.387
Cereb7 r (Cerebelum 7b Right)	2.063	5.825	0.627	3.936
Cereb8 l (Cerebelum 8 Left)	1.728	5.49	0.601	3.591
Cereb8 r (Cerebelum 8 Right)	1.85	5.522	0.592	4.503
Cereb9 l (Cerebelum 9 Left)	1.61	4.825	0.793	3.397
Cereb9 r (Cerebelum 9 Right)	1.787	5.12	0.786	3.752
Cereb10 l (Cerebelum 10 Left)	1.482	3.932	1.676	4.387
Cereb10 r (Cerebelum 10 Right)	2.252	5.251	1.468	2.874
Ver12 (Vermis 1 2)	0.722	2.147	1.42	2.733
Ver3 (Vermis 3)	2.339	5.212	1.026	2.733
Ver45 (Vermis 4 5)	2.071	5.204	2.062	4.648
Ver6 (Vermis 6)	2.372	4.831	1.875	3.455
Ver7 (Vermis 7)	2.233	4.619	1.984	3.993
Ver8 (Vermis 8)	2.821	5.331	1.869	3.641
Ver9 (Vermis 9)	1.538	3.272	1.856	3.621
Ver10 (Vermis 10)	1.484	3.478	0.749	2.834
Extended amygdala r	1.492	2.814	1.772	3.277
Extended amygdala l	0.805	2.524	0.926	2.469
Substantia nigra pars compacta r	2.074	4.026	0.649	3.198
Substantia nigra pars compacta l	1.934	3.382	0.571	2.23
Nucleus ruber r	1.317	3.745	1.493	2.454
Nucleus ruber l	1.649	3.038	0.783	2.419
Substantia nigra pars reticularis r	2.261	4.785	0.915	3.198
Substantia nigra pars reticularis l	1.877	2.969	0.716	2.568
Parabrachial pigmented nucleus r	1.683	3.257	0.823	3.198
Parabrachial pigmented nucleus l	2.03	3.352	0.481	1.851
Ventral tegmental area r	2.297	3.138	0.942	1.755
Ventral tegmental area l	1.499	2.507	0.95	1.851
Ventral pallidum r	0.994	1.736	0.549	1.528
Ventral pallidum l	0.65	2.519	1.504	2.555
Hypothalamus r	1.349	3.124	0.329	3.569
Hypothalamus l	1.602	3.754	1.033	2.383
Mammilary body r	1.062	2.335	2.594	3.368

Region (Harvard Oxford Atlas, extended)	This study		Rebollo (2018)	
	Mean *t*	**Max *t***	**Mean *t***	**Max *t***
Mammilary body l	1.949	2.872	1.509	2.752
Subthalamic nucleus r	1.89	2.668	0.624	1.903
Subthalamic nucleus l	2.253	3.902	0.305	2.383
NTS new r	1.252	2.842	0.136	1.905
NTS new l	1.191	3.006	0.081	2.704

Table S2. Related to Figure 2. Effect sizes per region.

	Baseline			taVNS > Sham		
Region (Harvard Oxford Atlas, extended)	**Mean d_z**	**Max d_z**	**Std d_z**	**Mean d_z**	**Max d_z**	**Std d_z**
FP r (Frontal Pole Right)	0.17	0.917	0.188	0.014	0.535	0.154
FP l (Frontal Pole Left)	0.247	0.736	0.161	0.024	0.765	0.158
IC r (Insular Cortex Right)	0.306	0.864	0.187	0.112	0.59	0.16
IC l (Insular Cortex Left)	0.352	0.966	0.186	0.119	0.609	0.163
SFG r (Superior Frontal Gyrus Right)	0.204	1.165	0.239	0.045	0.66	0.175
SFG l (Superior Frontal Gyrus Left)	0.273	0.978	0.171	-0.02	0.471	0.148
MidFG r (Middle Frontal Gyrus Right)	0.268	1.083	0.201	0.101	0.893	0.202
MidFG l (Middle Frontal Gyrus Left)	0.252	0.66	0.142	0.041	0.511	0.168
IFG tri r (Inferior Frontal Gyrus, pars triangularis Right)	0.34	0.801	0.146	0.033	0.62	0.175
IFG tri l (Inferior Frontal Gyrus, pars triangularis Left)	0.36	0.934	0.148	-0.036	0.422	0.139
IFG oper r (Inferior Frontal Gyrus, pars opercularis Right)	0.397	1.066	0.2	0.087	0.573	0.175
IFG oper l (Inferior Frontal Gyrus, pars opercularis Left)	0.368	0.746	0.131	-0.106	0.389	0.152
PreCG r (Precentral Gyrus Right)	0.424	1.045	0.154	-0.023	0.612	0.16
PreCG l (Precentral Gyrus Left)	0.401	1.065	0.155	-0.018	0.58	0.165
TP r (Temporal Pole Right)	0.211	0.93	0.169	0.009	0.751	0.174
TP l (Temporal Pole Left)	0.216	0.815	0.175	-0.064	0.606	0.187
aSTG r (Superior Temporal Gyrus, anterior division Right)	0.313	0.673	0.128	0.067	0.462	0.114
aSTG l (Superior Temporal Gyrus, anterior division Left)	0.214	0.799	0.135	-0.114	0.297	0.131
pSTG r (Superior Temporal Gyrus, posterior division Right)	0.236	0.538	0.133	-0.08	0.348	0.157
pSTG l (Superior Temporal Gyrus, posterior division Left)	0.127	0.566	0.141	-0.155	0.2	0.137
aMTG r (Middle Temporal Gyrus, anterior division Right)	0.206	0.459	0.094	0.098	0.411	0.119
aMTG l (Middle Temporal Gyrus, anterior division Left)	0.113	0.642	0.102	-0.015	0.439	0.15
pMTG r (Middle Temporal Gyrus, posterior division Right)	0.146	0.593	0.185	0.087	0.68	0.169
pMTG l (Middle Temporal Gyrus, posterior division Left)	0.139	0.562	0.143	-0.04	0.527	0.186
toMTG r (Middle Temporal Gyrus, temporooccipital part Right)	0.302	0.831	0.156	0.165	0.612	0.176
toMTG l (Middle Temporal Gyrus, temporooccipital part Left)	0.274	0.838	0.213	0.012	0.467	0.162
aITG r (Inferior Temporal Gyrus, anterior division Right)	0.377	0.794	0.204	0.076	0.462	0.151

	Baseline			taVNS > Sham		
Region (Harvard Oxford Atlas, extended)	**Mean d_z**	**Max d_z**	**Std d_z**	**Mean d_z**	**Max d_z**	**Std d_z**
aITG l (Inferior Temporal Gyrus, anterior division Left)	0.309	0.791	0.196	-0.024	0.565	0.149
pITG r (Inferior Temporal Gyrus, posterior division Right)	0.226	0.701	0.131	0.127	0.631	0.153
pITG l (Inferior Temporal Gyrus, posterior division Left)	0.256	0.79	0.149	0.08	0.578	0.14
toITG r (Inferior Temporal Gyrus, temporooccipital part Right)	0.371	0.893	0.221	0.096	0.608	0.171
toITG l (Inferior Temporal Gyrus, temporooccipital part Left)	0.373	0.954	0.183	0.098	0.485	0.143
PostCG r (Postcentral Gyrus Right)	0.416	1.023	0.142	0.001	0.494	0.164
PostCG l (Postcentral Gyrus Left)	0.379	0.909	0.146	-0.053	0.484	0.165
SPL r (Superior Parietal Lobule Right)	0.405	0.791	0.152	-0.014	0.487	0.157
SPL l (Superior Parietal Lobule Left)	0.426	1.068	0.174	-0.039	0.412	0.162
aSMG r (Supramarginal Gyrus, anterior division Right)	0.392	0.855	0.128	0.118	0.496	0.126
aSMG l (Supramarginal Gyrus, anterior division Left)	0.354	0.831	0.16	0.145	0.55	0.139
pSMG r (Supramarginal Gyrus, posterior division Right)	0.397	0.761	0.129	0.134	0.631	0.163
pSMG l (Supramarginal Gyrus, posterior division Left)	0.322	0.834	0.169	0.015	0.444	0.151
AG r (Angular Gyrus Right)	0.269	0.686	0.147	0.15	0.55	0.133
AG l (Angular Gyrus Left)	0.349	0.909	0.15	0.096	0.481	0.168
sLOC r (Lateral Occipital Cortex, superior division Right)	0.328	0.935	0.188	0.128	0.763	0.198
sLOC l (Lateral Occipital Cortex, superior division Left)	0.315	0.847	0.164	0.101	0.508	0.145
iLOC r (Lateral Occipital Cortex, inferior division Right)	0.434	0.838	0.114	-0.056	0.363	0.12
iLOC l (Lateral Occipital Cortex, inferior division Left)	0.373	0.714	0.139	-0.084	0.452	0.147
ICC r (Intracalcarine Cortex Right)	0.39	0.736	0.136	0.12	0.355	0.094
ICC l (Intracalcarine Cortex Left)	0.41	0.764	0.118	0.088	0.406	0.091
MedFC (Frontal Medial Cortex)	0.165	0.747	0.167	0.077	0.539	0.148
SMA r (Juxtapositional Lobule Cortex- Ri	0.387	0.906	0.16	0.044	0.413	0.131
SMA L(Juxtapositional Lobule Cortex- Lef	0.421	0.983	0.142	0.014	0.459	0.134
SubCalC (Subcallosal Cortex)	0.206	0.71	0.17	0.169	0.676	0.175
PaCiG r (Paracingulate Gyrus Right)	0.261	0.982	0.212	0.163	0.654	0.144

	Baseline			taVNS > Sham		
Region (Harvard Oxford Atlas, extended)	**Mean d_z**	**Max d_z**	**Std d_z**	**Mean d_z**	**Max d_z**	**Std d_z**
PaCiG l (Paracingulate Gyrus Left)	0.281	0.796	0.166	0.127	0.75	0.153
AC (Cingulate Gyrus, anterior division)	0.412	1.058	0.19	0.141	0.797	0.174
PC (Cingulate Gyrus, posterior division)	0.356	1.035	0.158	0.228	0.699	0.149
Precuneous (Precuneous Cortex)	0.387	1.04	0.126	0.169	0.762	0.17
Cuneal r (Cuneal Cortex Right)	0.288	0.703	0.119	0.069	0.392	0.111
Cuneal l (Cuneal Cortex Left)	0.326	0.615	0.076	0.045	0.385	0.117
FOrb r (Frontal Orbital Cortex Right)	0.186	0.736	0.168	0.078	0.709	0.189
FOrb l (Frontal Orbital Cortex Left)	0.231	0.911	0.167	0.116	0.604	0.173
aPaHC r (Parahippocampal Gyrus, anterior division Right)	0.298	1.185	0.22	0.045	0.518	0.159
aPaHC l (Parahippocampal Gyrus, anterior division Left)	0.281	0.91	0.152	0.02	0.398	0.148
pPaHC r (Parahippocampal Gyrus, posterior division Right)	0.343	0.687	0.139	0.06	0.459	0.178
pPaHC l (Parahippocampal Gyrus, posterior division Left)	0.263	0.712	0.163	0.042	0.395	0.174
LG r (Lingual Gyrus Right)	0.39	1.024	0.158	0.064	0.469	0.14
LG l (Lingual Gyrus Left)	0.324	0.818	0.144	0.095	0.608	0.15
aTFusC r (Temporal Fusiform Cortex, anterior division Right)	0.185	0.755	0.221	0.076	0.411	0.114
aTFusC l (Temporal Fusiform Cortex, anterior division Left)	0.23	0.6	0.155	-0.065	0.294	0.14
pTFusC r (Temporal Fusiform Cortex, posterior division Right)	0.341	0.843	0.146	0.147	0.553	0.151
pTFusC l (Temporal Fusiform Cortex, posterior division Left)	0.285	0.706	0.138	-0.004	0.554	0.181
TOFusC r (Temporal Occipital Fusiform Cortex Right)	0.459	1.229	0.155	0.089	0.548	0.139
TOFusC l (Temporal Occipital Fusiform Cortex Left)	0.388	0.738	0.144	0.14	0.528	0.146
OFusG r (Occipital Fusiform Gyrus Right)	0.46	0.969	0.158	0.027	0.405	0.113
OFusG l (Occipital Fusiform Gyrus Left)	0.462	0.931	0.107	0.1	0.387	0.117
FO r (Frontal Operculum Cortex Right)	0.35	0.758	0.159	0.118	0.523	0.149
FO l (Frontal Operculum Cortex Left)	0.354	0.756	0.136	0.162	0.594	0.193
CO r (Central Opercular Cortex Right)	0.472	0.925	0.141	0.176	0.551	0.136
CO l (Central Opercular Cortex Left)	0.392	0.937	0.171	0.113	0.549	0.131

	Baseline			taVNS > Sham		
Region (Harvard Oxford Atlas, extended)	**Mean d_z**	**Max d_z**	**Std d_z**	**Mean d_z**	**Max d_z**	**Std d_z**
PO r (Parietal Operculum Cortex Right)	0.394	0.776	0.15	0.048	0.335	0.119
PO l (Parietal Operculum Cortex Left)	0.457	0.901	0.139	-0.009	0.519	0.141
PP r (Planum Polare Right)	0.358	0.777	0.18	0.022	0.63	0.178
PP l (Planum Polare Left)	0.354	0.935	0.167	-0.028	0.633	0.211
HG r (Heschl's Gyrus Right)	0.433	0.842	0.141	0.171	0.511	0.133
HG l (Heschl's Gyrus Left)	0.389	0.907	0.149	0.076	0.376	0.118
PT r (Planum Temporale Right)	0.321	0.787	0.142	0.023	0.477	0.138
PT l (Planum Temporale Left)	0.297	0.766	0.174	-0.099	0.36	0.175
SCC r (Supracalcarine Cortex Right)	0.376	0.671	0.138	0.131	0.344	0.089
SCC l (Supracalcarine Cortex Left)	0.413	0.738	0.122	0.091	0.365	0.115
OP r (Occipital Pole Right)	0.352	0.83	0.136	0.065	0.367	0.111
OP l (Occipital Pole Left)	0.373	0.722	0.131	0.078	0.443	0.14
Thalamus r	0.465	1.006	0.163	0.038	0.614	0.141
Thalamus l	0.395	0.947	0.17	-0.008	0.444	0.153
Caudate r	0.159	0.563	0.146	-0.07	0.327	0.12
Caudate l	0.245	0.788	0.192	-0.052	0.234	0.124
Putamen r	0.254	0.683	0.148	-0.165	0.308	0.173
Putamen l	0.261	0.77	0.155	-0.158	0.229	0.152
Pallidum r	0.268	0.745	0.177	0.095	0.49	0.158
Pallidum l	0.331	0.931	0.186	0.096	0.542	0.182
Hippocampus r	0.285	0.771	0.161	-0.01	0.445	0.154
Hippocampus l	0.296	0.829	0.164	0.026	0.517	0.167
Amygdala r	0.299	0.726	0.136	-0.112	0.294	0.138
Amygdala l	0.291	0.612	0.121	-0.032	0.474	0.151
Accumbens r	0.228	0.508	0.123	0.076	0.345	0.136
Accumbens l	0.133	0.39	0.149	0.107	0.362	0.12
Brain-Stem	0.289	1.125	0.184	0.012	0.549	0.173
Cereb1 l (Cerebelum Crus1 Left)	0.252	0.883	0.156	0.121	0.564	0.143
Cereb1 r (Cerebelum Crus1 Right)	0.297	0.891	0.155	0.095	0.484	0.128
Cereb2 l (Cerebelum Crus2 Left)	0.256	1.001	0.179	0.113	0.457	0.113
Cereb2 r (Cerebelum Crus2 Right)	0.364	0.864	0.144	0.102	0.569	0.125
Cereb3 l (Cerebelum 3 Left)	0.27	0.635	0.138	0.26	0.607	0.155
Cereb3 r (Cerebelum 3 Right)	0.298	0.72	0.152	0.095	0.453	0.158
Cereb45 l (Cerebelum 4 5 Left)	0.294	0.782	0.151	0.117	0.579	0.164
Cereb45 r (Cerebelum 4 5 Right)	0.306	0.697	0.135	0.12	0.65	0.164
Cereb6 l (Cerebelum 6 Left)	0.331	0.841	0.174	0.153	0.533	0.154
Cereb6 r (Cerebelum 6 Right)	0.374	1.138	0.164	0.121	0.86	0.171
Cereb7 l (Cerebelum 7b Left)	0.376	0.875	0.173	0.088	0.444	0.133
Cereb7 r (Cerebelum 7b Right)	0.412	1.046	0.207	0.075	0.405	0.111
Cereb8 l (Cerebelum 8 Left)	0.321	0.986	0.177	0.059	0.476	0.143
Cereb8 r (Cerebelum 8 Right)	0.343	0.992	0.189	0.108	0.622	0.139
Cereb9 l (Cerebelum 9 Left)	0.289	0.867	0.192	0.049	0.697	0.167

	Baseline			taVNS > Sham		
Region (Harvard Oxford Atlas, extended)	**Mean d_z**	**Max d_z**	**Std d_z**	**Mean d_z**	**Max d_z**	**Std d_z**
Cereb9 r (Cerebelum 9 Right)	0.321	0.92	0.189	0.044	0.454	0.161
Cereb10 l (Cerebelum 10 Left)	0.287	0.706	0.143	0.054	0.443	0.133
Cereb10 r (Cerebelum 10 Right)	0.497	0.943	0.186	0.136	0.441	0.106
Ver12 (Vermis 1 2)	0.13	0.386	0.153	-0.04	0.329	0.165
Ver3 (Vermis 3)	0.42	0.936	0.221	0.202	0.556	0.155
Ver45 (Vermis 4 5)	0.372	0.935	0.168	0.108	0.603	0.186
Ver6 (Vermis 6)	0.426	0.868	0.154	0.09	0.529	0.196
Ver7 (Vermis 7)	0.401	0.83	0.136	0.082	0.4	0.122
Ver8 (Vermis 8)	0.507	0.957	0.197	0.018	0.466	0.139
Ver9 (Vermis 9)	0.276	0.588	0.12	0.17	0.623	0.125
Ver10 (Vermis 10)	0.267	0.625	0.144	0.073	0.495	0.195
Extended amygdala r	0.268	0.505	0.103	0.027	0.177	0.097
Extended amygdala l	0.145	0.453	0.148	-0.038	0.163	0.15
Substantia nigra pars compacta r	0.372	0.723	0.169	0.013	0.233	0.157
Substantia nigra pars compacta l	0.347	0.608	0.121	0.139	0.419	0.137
Nucleus ruber r	0.237	0.673	0.172	0.233	0.531	0.124
Nucleus ruber l	0.296	0.546	0.11	0.08	0.547	0.157
Substantia nigra pars reticularis r	0.406	0.859	0.167	0.07	0.423	0.168
Substantia nigra pars reticularis l	0.337	0.533	0.144	0.131	0.503	0.129
Parabrachial pigmented nucleus r	0.302	0.585	0.192	0.142	0.405	0.139
Parabrachial pigmented nucleus l	0.365	0.602	0.138	0.038	0.325	0.137
Ventral tegmental area r	0.413	0.564	0.112	0.084	0.237	0.112
Ventral tegmental area l	0.269	0.45	0.116	0.343	0.611	0.223
Ventral pallidum r	0.179	0.312	0.063	0.01	0.119	0.075
Ventral pallidum l	0.117	0.453	0.167	-0.162	0.134	0.134
Hypothalamus r	0.242	0.561	0.156	0.032	0.483	0.192
Hypothalamus l	0.288	0.674	0.192	0.053	0.36	0.168
Mammilary body r	0.191	0.419	0.133	0.045	0.179	0.114
Mammilary body l	0.35	0.516	0.105	-0.059	0.159	0.123
Subthalamic nucleus r	0.339	0.479	0.089	0.224	0.551	0.149
Subthalamic nucleus l	0.405	0.701	0.174	0.194	0.468	0.175
NTS new r	0.225	0.51	0.134	0.055	0.75	0.258
NTS new l	0.214	0.54	0.129	0.221	0.778	0.208

Table S3. Related to Figure 4. Correlation between changes in PLV and changes in hunger.

Region (Harvard Oxford Atlas, extended)	Mean *r*	Max *r*	Std *r*
FP r (Frontal Pole Right)	0.117	0.764	0.197
FP l (Frontal Pole Left)	0.159	0.686	0.204
IC r (Insular Cortex Right)	-0.11	0.359	0.163
IC l (Insular Cortex Left)	-0.085	0.351	0.16
SFG r (Superior Frontal Gyrus Right)	0.064	0.546	0.158
SFG l (Superior Frontal Gyrus Left)	0.14	0.622	0.203
MidFG r (Middle Frontal Gyrus Right)	0.051	0.512	0.193
MidFG l (Middle Frontal Gyrus Left)	0.174	0.617	0.178
IFG tri r (Inferior Frontal Gyrus, pars triangularis Right)	0.025	0.497	0.151
IFG tri l (Inferior Frontal Gyrus, pars triangularis Left)	0.141	0.518	0.134
IFG oper r (Inferior Frontal Gyrus, pars opercularis Right)	-0.102	0.339	0.169
IFG oper l (Inferior Frontal Gyrus, pars opercularis Left)	-0.009	0.409	0.18
PreCG r (Precentral Gyrus Right)	0.069	0.604	0.185
PreCG l (Precentral Gyrus Left)	0.034	0.547	0.164
TP r (Temporal Pole Right)	0.126	0.536	0.16
TP l (Temporal Pole Left)	0.11	0.566	0.162
aSTG r (Superior Temporal Gyrus, anterior division Right)	0.014	0.424	0.157
aSTG l (Superior Temporal Gyrus, anterior division Left)	-0.037	0.325	0.167
pSTG r (Superior Temporal Gyrus, posterior division Right)	0.017	0.417	0.159
pSTG l (Superior Temporal Gyrus, posterior division Left)	-0.024	0.361	0.164
aMTG r (Middle Temporal Gyrus, anterior division Right)	0.116	0.503	0.129
aMTG l (Middle Temporal Gyrus, anterior division Left)	0.121	0.462	0.148
pMTG r (Middle Temporal Gyrus, posterior division Right)	0.243	0.616	0.138
pMTG l (Middle Temporal Gyrus, posterior division Left)	0.172	0.558	0.162
toMTG r (Middle Temporal Gyrus, temporooccipital part Right)	0.043	0.514	0.214
toMTG l (Middle Temporal Gyrus, temporooccipital part Left)	0.045	0.528	0.173
aITG r (Inferior Temporal Gyrus, anterior division Right)	-0.003	0.385	0.169
aITG l (Inferior Temporal Gyrus, anterior division Left)	0.087	0.434	0.145
pITG r (Inferior Temporal Gyrus, posterior division Right)	0.105	0.541	0.176
pITG l (Inferior Temporal Gyrus, posterior division Left)	0.062	0.529	0.164

Region (Harvard Oxford Atlas, extended)	Mean *r*	Max *r*	Std *r*
toITG r (Inferior Temporal Gyrus, temporooccipital part Right)	0.301	0.622	0.148
toITG l (Inferior Temporal Gyrus, temporooccipital part Left)	0.345	0.627	0.147
PostCG r (Postcentral Gyrus Right)	0.098	0.611	0.17
PostCG l (Postcentral Gyrus Left)	0.094	0.491	0.157
SPL r (Superior Parietal Lobule Right)	0.045	0.519	0.19
SPL l (Superior Parietal Lobule Left)	0.121	0.568	0.217
aSMG r (Supramarginal Gyrus, anterior division Right)	-0.132	0.313	0.155
aSMG l (Supramarginal Gyrus, anterior division Left)	0.058	0.461	0.199
pSMG r (Supramarginal Gyrus, posterior division Right)	0.027	0.51	0.173
pSMG l (Supramarginal Gyrus, posterior division Left)	0.026	0.384	0.16
AG r (Angular Gyrus Right)	0.115	0.555	0.203
AG l (Angular Gyrus Left)	0.222	0.602	0.158
sLOC r (Lateral Occipital Cortex, superior division Right)	0.214	0.634	0.177
sLOC l (Lateral Occipital Cortex, superior division Left)	0.219	0.638	0.174
iLOC r (Lateral Occipital Cortex, inferior division Right)	0.25	0.561	0.173
iLOC l (Lateral Occipital Cortex, inferior division Left)	0.243	0.627	0.155
ICC r (Intracalcarine Cortex Right)	0.045	0.356	0.117
ICC l (Intracalcarine Cortex Left)	0.11	0.486	0.145
MedFC (Frontal Medial Cortex)	0.116	0.523	0.156
SMA r (Juxtapositional Lobule Cortex- Ri	0.039	0.458	0.136
SMA L(Juxtapositional Lobule Cortex- Lef	0.06	0.39	0.134
SubCalC (Subcallosal Cortex)	0.071	0.5	0.149
PaCiG r (Paracingulate Gyrus Right)	-0.089	0.483	0.192
PaCiG l (Paracingulate Gyrus Left)	0.024	0.56	0.177
AC (Cingulate Gyrus, anterior division)	-0.139	0.389	0.141
PC (Cingulate Gyrus, posterior division)	0.119	0.608	0.216
Precuneous (Precuneous Cortex)	0.138	0.622	0.179
Cuneal r (Cuneal Cortex Right)	-0.082	0.356	0.096
Cuneal l (Cuneal Cortex Left)	-0.11	0.184	0.129
FOrb r (Frontal Orbital Cortex Right)	0.077	0.48	0.171
FOrb l (Frontal Orbital Cortex Left)	0.009	0.417	0.158
aPaHC r (Parahippocampal Gyrus, anterior division Right)	0.101	0.536	0.178
aPaHC l (Parahippocampal Gyrus, anterior division Left)	0.041	0.445	0.161
pPaHC r (Parahippocampal Gyrus, posterior division Right)	0.034	0.445	0.172
pPaHC l (Parahippocampal Gyrus, posterior division Left)	0.079	0.424	0.138
LG r (Lingual Gyrus Right)	0.056	0.473	0.142
LG l (Lingual Gyrus Left)	0.07	0.461	0.137

Region (Harvard Oxford Atlas, extended)	Mean *r*	Max *r*	Std *r*
aTFusC r (Temporal Fusiform Cortex, anterior division Right)	0.135	0.509	0.136
aTFusC l (Temporal Fusiform Cortex, anterior division Left)	-0.024	0.299	0.131
pTFusC r (Temporal Fusiform Cortex, posterior division Right)	0.105	0.52	0.157
pTFusC l (Temporal Fusiform Cortex, posterior division Left)	0.111	0.456	0.148
TOFusC r (Temporal Occipital Fusiform Cortex Right)	0.269	0.645	0.149
TOFusC l (Temporal Occipital Fusiform Cortex Left)	0.185	0.552	0.117
OFusG r (Occipital Fusiform Gyrus Right)	0.204	0.552	0.138
OFusG l (Occipital Fusiform Gyrus Left)	0.197	0.585	0.118
FO r (Frontal Operculum Cortex Right)	-0.178	0.186	0.148
FO l (Frontal Operculum Cortex Left)	-0.087	0.355	0.177
CO r (Central Opercular Cortex Right)	-0.105	0.421	0.135
CO l (Central Opercular Cortex Left)	-0.126	0.317	0.124
PO r (Parietal Operculum Cortex Right)	-0.126	0.211	0.136
PO l (Parietal Operculum Cortex Left)	-0.13	0.301	0.125
PP r (Planum Polare Right)	0.059	0.486	0.176
PP l (Planum Polare Left)	0.026	0.381	0.158
HG r (Heschl's Gyrus Right)	-0.037	0.3	0.127
HG l (Heschl's Gyrus Left)	-0.057	0.308	0.125
PT r (Planum Temporale Right)	-0.104	0.31	0.147
PT l (Planum Temporale Left)	-0.065	0.429	0.131
SCC r (Supracalcarine Cortex Right)	-0.028	0.237	0.116
SCC l (Supracalcarine Cortex Left)	-0.013	0.24	0.112
OP r (Occipital Pole Right)	0.133	0.513	0.15
OP l (Occipital Pole Left)	0.121	0.449	0.163
Thalamus r	0.076	0.56	0.181
Thalamus l	0.067	0.573	0.157
Caudate r	0.012	0.495	0.153
Caudate l	0.058	0.411	0.149
Putamen r	0.06	0.392	0.162
Putamen l	0.093	0.534	0.156
Pallidum r	-0.031	0.412	0.177
Pallidum l	0.144	0.538	0.154
Hippocampus r	0.151	0.504	0.168
Hippocampus l	0.1	0.545	0.141
Amygdala r	0.055	0.482	0.166
Amygdala l	-0.007	0.458	0.175
Accumbens r	0.07	0.346	0.151
Accumbens l	0.064	0.387	0.153
Brain-Stem	0.044	0.571	0.16
Cereb1 l (Cerebelum Crus1 Left)	0.153	0.567	0.155
Cereb1 r (Cerebelum Crus1 Right)	0.228	0.684	0.17
Cereb2 l (Cerebelum Crus2 Left)	0.227	0.551	0.17
Cereb2 r (Cerebelum Crus2 Right)	0.291	0.632	0.164
Cereb3 l (Cerebelum 3 Left)	-0.094	0.21	0.129
Cereb3 r (Cerebelum 3 Right)	-0.023	0.326	0.169

Region (Harvard Oxford Atlas, extended)	Mean *r*	Max *r*	Std *r*
Cereb45 l (Cerebelum 4 5 Left)	-0.02	0.36	0.137
Cereb45 r (Cerebelum 4 5 Right)	-0.008	0.352	0.151
Cereb6 l (Cerebelum 6 Left)	0.079	0.507	0.169
Cereb6 r (Cerebelum 6 Right)	0.079	0.438	0.149
Cereb7 l (Cerebelum 7b Left)	0.133	0.579	0.236
Cereb7 r (Cerebelum 7b Right)	0.199	0.527	0.173
Cereb8 l (Cerebelum 8 Left)	0.053	0.49	0.158
Cereb8 r (Cerebelum 8 Right)	0.101	0.569	0.156
Cereb9 l (Cerebelum 9 Left)	0.073	0.478	0.175
Cereb9 r (Cerebelum 9 Right)	0.042	0.457	0.183
Cereb10 l (Cerebelum 10 Left)	0.165	0.483	0.16
Cereb10 r (Cerebelum 10 Right)	-0.049	0.459	0.186
Ver12 (Vermis 1 2)	-0.117	0.235	0.144
Ver3 (Vermis 3)	-0.027	0.387	0.157
Ver45 (Vermis 4 5)	-0.053	0.335	0.162
Ver6 (Vermis 6)	0.016	0.38	0.135
Ver7 (Vermis 7)	0.099	0.45	0.189
Ver8 (Vermis 8)	0.047	0.385	0.113
Ver9 (Vermis 9)	0.139	0.435	0.121
Ver10 (Vermis 10)	0.059	0.421	0.216
Extended amygdala r	0.093	0.218	0.075
Extended amygdala l	-0.015	0.23	0.155
Substantia nigra pars compacta r	0.042	0.24	0.114
Substantia nigra pars compacta l	-0.003	0.314	0.125
Nucleus ruber r	-0.02	0.423	0.186
Nucleus ruber l	0.142	0.48	0.134
Substantia nigra pars reticularis r	0.041	0.264	0.1
Substantia nigra pars reticularis l	0.112	0.416	0.183
Parabrachial pigmented nucleus r	-0	0.244	0.104
Parabrachial pigmented nucleus l	0.015	0.174	0.107
Ventral tegmental area r	0.095	0.223	0.143
Ventral tegmental area l	0.075	0.211	0.102
Ventral pallidum r	-0.127	0.035	0.082
Ventral pallidum l	-0.03	0.119	0.122
Hypothalamus r	0.029	0.382	0.145
Hypothalamus l	0.04	0.387	0.167
Mammilary body r	-0.163	-0.035	0.107
Mammilary body l	-0.074	0.255	0.211
Subthalamic nucleus r	0.126	0.388	0.103
Subthalamic nucleus l	0.041	0.251	0.136
NTS new r	0.095	0.461	0.145
NTS new l	-0.137	0.197	0.126

References (SI)

Avants, B. B., Epstein, C. L., Grossman, M., & Gee, J. C. (2008). Symmetric diffeomorphic image registration with cross-correlation: evaluating automated labeling of elderly and neurodegenerative brain. *Med Image Anal*, *12*(1), 26-41. https://doi.org/10.1016/j.media.2007.06.004

Birn, R. M., Smith, M. A., Jones, T. B., & Bandettini, P. A. (2008). The respiration response function: the temporal dynamics of fMRI signal fluctuations related to changes in respiration. *Neuroimage*, *40*(2), 644-654. https://doi.org/10.1016/j.neuroimage.2007.11.059

Cox, R. W. (1996). AFNI: software for analysis and visualization of functional magnetic resonance neuroimages. *Comput Biomed Res*, *29*(3), 162-173. https://doi.org/10.1006/cbmr.1996.0014

Dale, A. M., Fischl, B., & Sereno, M. I. (1999). Cortical surface-based analysis. I. Segmentation and surface reconstruction. *Neuroimage*, *9*(2), 179-194. https://doi.org/10.1006/nimg.1998.0395

Fonov, V. S., Evans, A. C., McKinstry, R. C., Almli, C. R., & Collins, D. L. (2009). Unbiased nonlinear average age-appropriate brain templates from birth to adulthood. *Neuroimage*, *47*, S102. https://doi.org/https://doi.org/10.1016/S1053-8119(09)70884-5

Greve, D. N., & Fischl, B. (2009). Accurate and robust brain image alignment using boundary-based registration. *Neuroimage*, *48*(1), 63-72. https://doi.org/10.1016/j.neuroimage.2009.06.060

Jenkinson, M. (2003). Fast, automated, N-dimensional phase-unwrapping algorithm. *Magn Reson Med*, *49*(1), 193-197. https://doi.org/10.1002/mrm.10354

Jenkinson, M., Bannister, P., Brady, M., & Smith, S. (2002). Improved optimization for the robust and accurate linear registration and motion correction of brain images. *Neuroimage*, *17*(2), 825-841. https://doi.org/10.1016/s1053-8119(02)91132-8

Kasper, L., Bollmann, S., Diaconescu, A. O., Hutton, C., Heinzle, J., Iglesias, S., Hauser, T. U., Sebold, M., Manjaly, Z. M., Pruessmann, K. P., & Stephan, K. E. (2017). The PhysIO Toolbox for Modeling Physiological Noise in fMRI Data. *J Neurosci Methods*, *276*, 56-72. https://doi.org/10.1016/j.jneumeth.2016.10.019

Klein, A., Ghosh, S. S., Bao, F. S., Giard, J., Hame, Y., Stavsky, E., Lee, N., Rossa, B., Reuter, M., Chaibub Neto, E., & Keshavan, A. (2017). Mindboggling morphometry of human brains. *PLoS Comput Biol*, *13*(2), e1005350. https://doi.org/10.1371/journal.pcbi.1005350

Margulies, D. S., Ghosh, S. S., Goulas, A., Falkiewicz, M., Huntenburg, J. M., Langs, G., Bezgin, G., Eickhoff, S. B., Castellanos, F. X., Petrides, M., Jefferies, E., & Smallwood, J. (2016). Situating the default-mode network along a principal gradient of macroscale cortical organization. *Proc Natl Acad Sci U S A*, *113*(44), 12574-12579. https://doi.org/10.1073/pnas.1608282113

Oostenveld, R., Fries, P., Maris, E., & Schoffelen, J. M. (2011). FieldTrip: Open source software for advanced analysis of MEG, EEG, and invasive electrophysiological data. *Comput Intell Neurosci*, *2011*, 156869. https://doi.org/10.1155/2011/156869

Power, J. D., Mitra, A., Laumann, T. O., Snyder, A. Z., Schlaggar, B. L., & Petersen, S. E. (2014). Methods to detect, characterize, and remove motion artifact in resting state fMRI. *Neuroimage*, *84*, 320-341. https://doi.org/10.1016/j.neuroimage.2013.08.048

Rebollo, I., Devauchelle, A. D., Beranger, B., & Tallon-Baudry, C. (2018). Stomach-brain synchrony reveals a novel, delayed-connectivity resting-state network in humans. *Elife*, *7*. https://doi.org/10.7554/eLife.33321

Teckentrup, V., Krylova, M., Jamalabadi, H., Neubert, S., Neuser, M. P., Hartig, R., Fallgatter, A. J., Walter, M., & Kroemer, N. B. (2021). Brain signaling dynamics after vagus nerve stimulation. *Neuroimage*, *245*, 118679. https://doi.org/https://doi.org/10.1016/j.neuroimage.2021.118679

Tustison, N. J., Avants, B. B., Cook, P. A., Zheng, Y., Egan, A., Yushkevich, P. A., & Gee, J. C. (2010). N4ITK: improved N3 bias correction. *IEEE Trans Med Imaging*, *29*(6), 1310-1320. https://doi.org/10.1109/TMI.2010.2046908

Wolpert, N., Rebollo, I., & Tallon-Baudry, C. (2020). Electrogastrography for psychophysiological research: Practical considerations, analysis pipeline, and normative data in a large sample. *Psychophysiology*, *57*(9), e13599. https://doi.org/10.1111/psyp.13599

Yeo, B. T., Krienen, F. M., Sepulcre, J., Sabuncu, M. R., Lashkari, D., Hollinshead, M., Roffman, J. L., Smoller, J. W., Zollei, L., Polimeni, J. R., Fischl, B., Liu, H., & Buckner, R. L. (2011). The organization of the human cerebral cortex estimated by intrinsic functional connectivity. *J Neurophysiol*, *106*(3), 1125-1165. https://doi.org/10.1152/jn.00338.2011

Zhang, Y., Brady, M., & Smith, S. (2001). Segmentation of brain MR images through a hidden Markov random field model and the expectation-maximization algorithm. *IEEE Trans Med Imaging*, *20*(1), 45-57. https://doi.org/10.1109/42.906424